NASA TT F-10,219

INVESTIGATION OF WALL SURFACE TEMPERATURE BEHIND A MOVING SHOCK WAVE

M.V. Volodina, Yu.A. Dem'yanov,
S.S. Kellin, N.V. Chereshneva

NASA TT F-10,219

FACILITY FORM 602

N66 33678 (ACCESSION NUMBER) | (THRU)

11 (PAGES) | 1 (CODE)

(NASA CR OR TMX OR AD NUMBER) | 33 (CATEGORY)

Translation of "Issledovaniye Temperatury Poverkhnosti Stenki za Dvizhushcheysya udarnoy volnoy".
Izvestiya Akademii Nauk SSSR, Otdeleniye Tekhnicheskikh Nauk, Mekhanika i Mashinostroyeniye, No. 6, pp 112-116, 1960

NATIONAL AERONAUTICS AND SPACE ADMINISTRATION
WASHINGTON D.C. JUNE 1966

NASA TTF-10,219

INVESTIGATION OF WALL SURFACE TEMPERATURE BEHIND A MOVING SHOCK WAVE

M. V. Volodina, Yu. A. Dem'yanov
S. S. Kellin, N. V. Chereshneva

(Moscow)

ABSTRACT

33678

The wall surface temperature behind a moving shock wave is determined experimentally and theoretically. The non-stationary boundary layer equations are solved for a plate, for constant flux behind the shock wave. Experiment and theory agree to within the experimental accuracy ($\pm$ 10-15%).

A theoretical and experimental investigation of wall surface temperature behind a shock wave moving at a constant velocity is presented. /112*

The wall surface temperature is determined from the equation of heat balance (radiant heat exchange is not taken into account) under the condition that the temperature of the gas and the wall are the same on the surface.

In order to compute the convective thermal flux, the equations of a non-stationary boundary layer of a compressible gas are solved for a plate, when the flux velocity behind the shock wave U_∞ is constant. The thermal flux at the wall is found by solving the thermal conductivity equation.

As follows from (Ref. 1), the boundary layer in the region behind the shock wave will be stationary, under the assumption that the wall temperature is constant. The latter statement is verified in (Ref. 2), and it will also be verified by the statements which follow, if it is assumed that the flux composition does not change behind the moving shock wave.

* Note: Numbers in the margin indicate pagination in the original foreign text.

In view of the large range over which the temperatures change in the boundary layer, allowance must be made for the deviation of the viscosity law from the usually accepted law $\mu\rho$ = const, for the variability of the Prandtl number $\sigma = \mu c_p/\lambda$ with temperature, and also for the phenomenon of diffusion. We should point out that the phenomenon of diffusion has no significant influence on the thermal flux for the case considered below, due to the fact that the Prandtl diffusion number is close to one and that the concentration gradient is small in the boundary layer region close to the wall (lower wall temperatures).

The following may be used as the initial system of equations for solving this problem:

$$g(u)\,g''(u) = -uf(i)$$

$$\left[\frac{1}{\sigma} i'(u)\right]' + \frac{g'(u)}{g(u)}\left(\frac{1}{\sigma} - 1\right) i'(u) + c = 0 \qquad \tau = \frac{g(u)}{\sqrt{2x}} \tag{1}$$

This is obtained from the equation for a laminar, stationary (in the system of coordinates related to the shock wave) boundary layer in the Crocco form for the dimensionless values:

$$u = \frac{u^\circ}{U}, \quad \tau = \frac{\tau^\circ}{\rho_\infty U^2}, \quad i = \frac{i^\circ}{i_\infty} \quad \left(\tau^\circ = \mu^\circ \frac{\partial u^\circ}{\partial y^\circ} = X(x)\,g(u)\right)$$

$$x = \frac{x^\circ \rho_\infty U}{\mu_\infty}, \quad f = \frac{\mu^\circ \rho^\circ}{\mu_\infty \rho_\infty}, \quad c = \frac{U^2}{i_\infty}$$

for the following boundary conditions:

$$g'(u) = 0, \quad i = i_w \quad \text{for} \quad u = 1;$$
$$g(u) = 0, \quad i = 1 \quad \text{for} \quad u = 1 - \frac{U_\infty}{U} \tag{2}$$

Here u° is an arbitrary velocity component; U - the shock wave velocity; τ° - friction stress (Ref. 3); $i^\circ = i^\circ(u)$ - enthalpy (Ref. 3); μ°, ρ° - viscosity and density, respectively.

The index ∞ is used to designate the parameters on the outer boundary of the boundary layer.

The solution of system (1) by the successive approximation method assumes the following form

$$g_1(u) = -\int_{u^*}^{u} du_1 \int_{1}^{u_1} \frac{f(i_0) - 1}{g_0(u)} u\,du, \quad i(u) = 1 - c\sigma J_1(u, u^*) + eJ_2(u, u^*) \qquad (3)$$

where i_0 and τ_0 represent the exact solutions of the boundary layer equation in the case of $\sigma = 1$ and $f = \text{const} = 1$

$$u^* = 1 - \frac{U_\infty}{U}, \qquad J_1(u, u^*) = \int_{u^*}^{u} g^{\sigma-1} du_1 \int_{1}^{u_1} g^{1-\sigma} du, \qquad J_2(u, u^*) = \int_{u^*}^{u} g^{\sigma-1} du.$$

Thus, the expression for the convective thermal flux may be written as follows

$$q_w = -\frac{i_\infty}{\sigma_w \sqrt{2}} \sqrt{\frac{\rho_\infty \mu_\infty U}{x}}\, g(1)\, e\, |g(1)|^{\sigma_w - 1} = \frac{Q\sqrt{U}}{\sqrt{x}} \qquad (4)$$

where

$$e = -\frac{i_w - 1 + c\sigma J_1(1, u^*)}{J_2(1, u^*)}$$

/113

In order to compute the functions $g_0(u)$ and $g_0'(u)$, whose form is given in Figure 1, we may employ the following formulas

$$g_0(u) = -\sqrt{2}\Phi_0''(\xi), \qquad g_0'(u) = \frac{1}{\sqrt{2}}[\Phi_0(\xi) - \xi], \qquad (5)$$
$$u = 1 - \Phi_0'(\xi)$$

The values of the functions $\Phi_0(\xi)$ and $\Phi_0''(\xi)$, are given in Table 1; the values of the function $\Phi_0'(\xi)$ are tabulated in (Ref. 1).

We should note that the functions $\Phi_0(\S)$ depend on $\Phi_0''(0)$ which determines the parameter U_∞/U.

Formula (4) for convective thermal flux at a certain point on the wall surface may be written as follows:

$$q_w(t) = \frac{Q}{\sqrt{t}} \qquad (6)$$

where the time t is computed from the moment the shock wave arrives at this point.

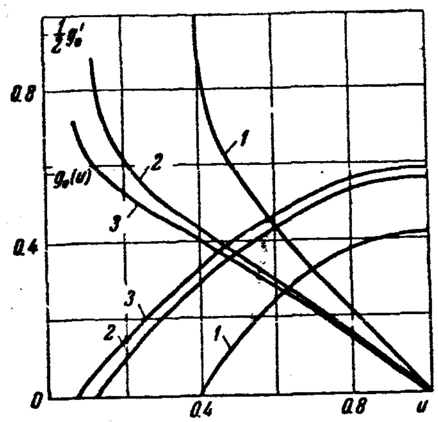

Figure 1

1 - $\Phi_0''(0) = 0.3$; 2 - $\Phi_0''(0) = 0.4$; 3 - $\Phi_0''(0) = 0.42$.

The form of the latter formula substantiates the assumption regarding the uniform temperature of the wall surface, since the thermal flux at the wall (assumed to be a semi-limited space) changes according to a similar law:

$$q_w(t) = \frac{\lambda (T_w - T_{w0})}{\sqrt{\pi a_0 t}} \tag{7}$$

where λ, a_0, T_{w0} are the coefficients of thermal conductivity and temperature conductivity of the wall material, and the initial temperature of the wall surface, respectively.

The following equation is obtained from (6) and (7) in order to determine the wall surface temperature T_w at the moment the shock wave passes:

$$T_w - T_{w0} = \frac{\sqrt{\pi a_0}}{\lambda} Q \tag{8}$$

or

$$\varphi(U) = \frac{\lambda \Delta T}{i_\infty \sqrt{\pi a_0 \rho_\infty \mu_\infty}} = -\frac{g(1) e \mid g(1) \mid^{\sigma_w - 1}}{\sqrt{2\sigma_w}} = A$$

In view of the smallness of the temperature jump $T_w - T_{w0}$ and the slight dependence of Q on T_w, the value of A may be computed according to the temperature T_{w0}. When necessary, the value of Q may be readily determined more

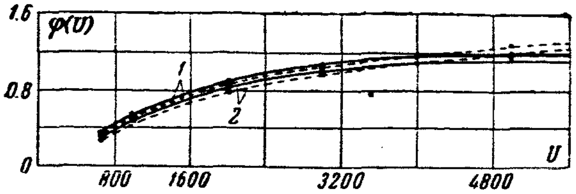

Figure 2

1- $\mu\rho \neq$ const, $\sigma = 0.72$; 2- $\mu\rho \neq$ const: $\sigma = 1$

accurately on the basis of the value found for T_w.

Figure 2 presents a graph showing the dependence of $\phi(U)$ on the shock wave velocity U calculated for $\Phi_0''(0) = 0.3, 0.4, 0.42$ in the case of the power law of viscosity

$$\frac{\mu^\circ\rho^\circ}{\mu_\infty\rho_\infty} = \left(\frac{i^\circ}{i_\infty}\right)^{n-1}$$

for the value of $n = 0.75$, which is usually assumed.

The deviation of this viscosity law from the existing data on viscosity for air in a large temperature range of 0 - 6000°C is 4%.

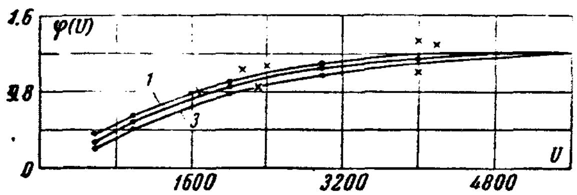

Figure 3

1- T_{w0} = 300°K; 2- T_{w0} = 400°K; 3- T_{w0} = 600°K, × - Experiment Results

/114

Certain computational results for T_{w0} = 300, 400 and 600°K and $\sigma = 0.72$ are shown in Figure 3. The study (Ref. 4) presents the extrapolation formula

$$-\frac{f''(0)}{V-1} = \frac{i'(0)}{i-i_w}\sigma^{-(0.48+0.022V)} = 0.489\sqrt{1+1.665V}\,(c_e)^{0.29}$$

which was verified for $\sigma = 1$. Figure 2 presents the dependence

$$\varphi(U) = \sigma_w^{0.022V-0.52}\left[1-\frac{i_\infty}{i_e}+\frac{V_\infty^2}{2i_e}\sigma_w^{0.39-0.023V}\right]0.489\sqrt{1+1.665V}\,c_e^{-0.21}\sqrt{\frac{1}{2V}} \qquad (9)$$

obtained by recalculating the formulas in (Ref. 4) in accordance with formula (8) for the viscosity law in the following form

$$c = \frac{\mu^\circ \rho^\circ}{\mu_\infty \rho_\infty} = \frac{1.5481}{i/i_w} - \frac{0.5481}{\sqrt{i/i_w}} + $$
$$+ 0.0028\left(\frac{i}{i_w} - 1\right) - 5.74 \cdot 10^{-5}\left(\frac{i}{i_w} - 1\right)^2$$

Here

$$\frac{i}{i_w} = \left[1 - \frac{u_e^2}{2H_e} f'^2\right]\left[1 - \frac{u_e^2}{2H_e} V^2\right]^{-1}$$
$$\left(H_e = i_e + \frac{u_e^2}{2},\ f' = \frac{u}{u_e},\ V = \frac{u_w}{u_e}\right)$$

where i is statistical enthalpy, and H_e is damping enthalpy.

A comparison of the two curves shown in Figure 2 shows that the difference in the solutions does not exceed 5 - 9%.

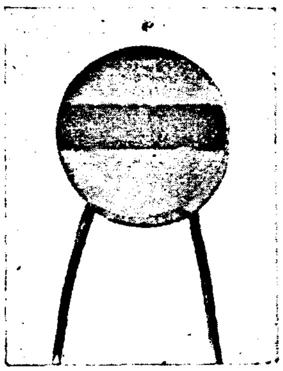

Figure 4.

Resistance Thermometer
(Recorder)

The temperature of the wall surface was measured by film resistance /115
thermometers.

The recorder is shown in Figure 4. A metallic, or semiconducting film is its sensitive element (nickel, stannic oxide, etc.) with dimensions of 1 x 5mm; this is located on a cylindrical base made of molybdenum glass.

The thickness of the metallic films is 0.1 - 0.5 microns; the films made

TABLE 1

/114

$\Phi_0''(0) = 0.42$

ξ	Φ_0	Φ_0'	Φ_0''	ξ	Φ_0	Φ_0'	Φ_0''
0	0.0000	0.0000	0.4200	3.9	2.2283	0.8725	0.0474
0.1	0.0021	0.0420	0.4190	4.0	2.3158	0.8771	0.0437
0.2	0.0034	0.0837	0.4159	4.2	2.4919	0.8858	0.0367
0.3	0.0188	0.1251	0.4110	4.4	2.6697	0.8927	0.0309
0.4	0.0330	0.1660	0.4046	4.5	2.8488	0.8984	0.0259
0.5	0.0512	0.2061	0.3966	4.8	3.0289	0.9032	0.0217
0.6	0.0734	0.2454	0,3871	5.0	3.2099	0.9072	0.0182
0.7	0.0995	0.2837	0.3765	5.2	3.3917	0.9106	0.0152
0.8	0.1293	0.3209	0.3648	5.4	3.5741	0.9134	0.0126
0.9	0.1629	0.3569	0.3522	5.6	3.7570	0.9157	0.0105
1.0	0.1999	0.3916	0.3390	5.8	3.9403	0.9176	0.0087
1.2	0.2843	0.4569	0.3112	6.0	4.1239	0.9192	0.0072
1.4	0.3811	0.5166	0.2825	6.2	4.3079	0.9206	0.0060
1.6	0.4794	0.5705	0.2539	6.4	4.4921	0.9217	0.0049
1.8	0.5979	0.6187	0.2260	6.6	4.6765	0.9226	0.0041
2.0	0.7256	0.6615	0.1997	7.02	5.0643	0.9240	0.0026
2.1	0.7940	0.6810	0.1872	7.22	5.2491	0.9244	0.0021
2.2	0.8628	0.6992	0.1753	7.42	5.4341	0.9248	0.0017
2.3	0.9334	0.7163	0.1638	7.62	5.6191	0.9252	0.0014
2.4	1.0058	0.7344	0.1529	7.82	5.8041	0.9254	0.0012
2.5	1.0799	0.7491	0.1424	8.1	6.0633	0.9257	0.0009
2.6	1.1553	0.7627	0.1325	8.22	6.1744	0.9258	0.0008
2.7	1.2321	0.7756	0.1231	8.46	6.3966	0.9260	0.0006
2.8	1.3102	0.7876	0.1143	8.62	6.5447	0.9261	0.0005
2.9	1.3894	0.7986	0.1060	8.86	6.7670	0.9262	0.0004
3.0	1.4697	0.8089	0.0982	9.1	6.9893	0.9263	0.0003
3.1	1.5509	0.8184	0.0908	9.26	7.1375	0.9263	0.0002
3.2	1.6331	0.8273	0.0840	9.66	7.5081	0.9264	0.0002
3.3	1.7162	0.8354	0,0776	9.82	7.6563	0.9264	0.0001
3.4	1.8000	0.8429	0.0716	10.06	7.8786	0.9265	0.0001
3.5	1.8846	0.8498	0.0660	10.30	8.1010	0.9265	0.0001
3.6	1.9699	0.8562	0.0608	10.62	8.3974	0.9265	0.0001
3.7	2.0557	0.8621	0.0560	10.70	8.4772	0.9265	0.0000
3.8	2.1414	0.8675	0.0516	10.94	8.6939	0.9265	0.0000

of stannic oxide are not as thick.

The initial film resistance is 10 - 1000 ohms for the different materials. The recorder is located flush with the wall surface, and is oriented lengthwise across the flux. (The influence of the ionized gas stream upon the film was taken into account during the experiments).

The signal $\Delta u = IR_0\alpha\Delta T$ was produced at the recorder during the thermal interaction on the film, where I is the recorder power current, R_0 - initial recorder resistance, and α - temperature coefficient of the film material resistance.

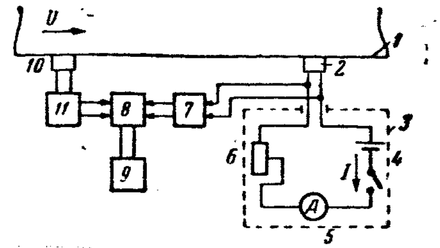

Figure 5

Block Diagram of Measurements.

1- Plate; 2- Resistance Thermometer; 3- Recorder Power System; 4- Power Supply; 5- Ammeter; 6- Instrument Multiplier; 7- Wide Band Preamplifier; 8- OK-17M Oscillograph; 9- Camera; 10- Starting Recorder; 11- Trigger Circuit.

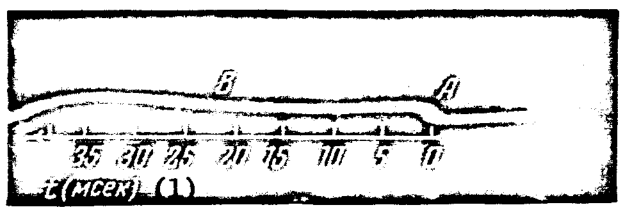

a /116

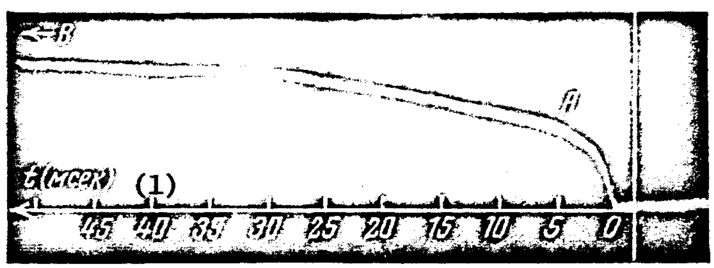

b

Figure 6

a- Pressure Before the Jump p = 1 mm Hg; b- Pressure before the Jump p = 10 mm Hg. (1) - msec.

The value of α was determined from the dependence $R = f(T)$, recorded in the thermostat for each recorder.

An electronic oscillograph was employed to record the signal from the

TABLE 2

$\Phi_0''(0) = 0.3$

ξ	Φ_0	Φ_0''	ξ	Φ_0	Φ_0''	ξ	Φ_0	Φ_0''
0	0.0000	0.3000	1.41	0.2749	0.1957	3.61	1.3896	0.0294
0.1	0.0015	0.2992	1.51	0.3126	0.1846	3.81	1.5068	0.0234
0.2	0.0060	0.9263	1.61	0.3522	0.1736	4.00	1.6191	0.0187
0.3	0.0134	0.2935	1.71	0.3935	0.1629	4.40	1.8575	0.0114
0.4	0.0238	0.2887	1.81	0.4453	0.1502	5.20	2.3400	0.0038
0.5	0.0371	0.2826	1.91	0.4810	0.1420	5.60	2.5821	0.0021
0.6	0.0532	0.2756	2.01	0.5270	0.1320	6.00	2.8245	0.0011
0.7	0.0721	0.2676	2.21	0.6229	0.1131	6.20	2.9458	0.0008
0.8	0.0936	0.2589	2.41	0.7233	0.0960	6.40	3.0671	0.0006
0.9	0.1178	0.2494	2.61	0.8277	0.0806	6.60	3.1885	0.0004
1.0	0.1444	0.2394	2.81	0.9353	0.0670	6.80	3.3098	0.0003
1.11	0.1741	0.2286	3.01	1.0465	0.0552	7.00	3.4312	0.0002
1.21	0.2055	0.2178	3.21	1.1591	0.0452	7.04	3.4555	0.0002
1.31	0.2391	0.2068	3.41	1.2736	0.0366	7.12	3.5040	0.0001
						7.16		0.0000

$\Phi_0''(0) = 0.4$

ξ	Φ_0	Φ_0''	ξ	Φ_0	Φ_0''	ξ	Φ_0	Φ_0''
0	0.0000	0.4000	1.7	0.5212	0.2272	4.4	2.5491	0.0282
0.4	0.0314	0.3853	1.8	0.5787	0.2139	4.8	2.8904	0.0192
0.5	0.0488	0.3776	1.9	0.6384	0.2010	5.2	3.2350	0.0129
0.6	0.0699	0.3686	2.0	0.7002	0.1934	5.6	3.5818	0.0086
0.7	0.0947	0.3584	2.2	0.8294	0.1691	6.4	4.2792	0.0037
0.8	0.1232	0.347[illegible]	2.4	0.9655	0.1469	6.8	4.6289	0.0024
0.9	0.1551	[illegible]	2.6	1.1076	0.1268	7.2	4.9790	0.0015
1.0	0.1904	0.3224	2.8	1.2547	0.1088	7.6	5.3294	0.0009
1.1	0.2290	0.3097	3.0	1.4063	0.0958	8.0	5.6800	0.0006
1.2	0.2707	0.2961	3.2	1.5619	0.0815	8.4	6.0306	0.0004
1.3	0.3154	0.2823	3.4	1.7207	0.0689	8.8	6.4164	0.0002
1.4	0.3629	0.2684	3.6	1.8824	0.0581	9.0	6.5567	0.0002
1.5	0.4131	0.2545	3.8	2.0464	0.0488	9.2	6.7321	0.0001
1.6	0.4659	0.2407	4.0	2.2124	0.0408	9.3	6.8198	0.0001
						9.4	6.9075	0.0000

recorder. Figure 5 shows a diagram of the measurements. Characteristic oscillograms of the wall temperature measurement with time are shown in Figure 6. The results derived from processing these measurements are plotted in Figure 3 with the computational results. The experimental points were obtained for the values of ΔT, corresponding to the time at which a flux with constant temperature (section AB) passed. The temperature increase in the initial section (1 - 5 microseconds), which had an influence upon the subsequent pattern of the curve, is apparently related both to the nonequilibrium phenomena behind the shock wave and to the transitional processes of the measurement apparatus.

The deviation of the experimental points from the computed curve is ± (10-15%), which comprises the accuracy of the experimental measurements.

Received May 26, 1960

REFERENCES

1. Dem'yanov, Y.A. Formation of the Boundary Layer on a Plate with a Moving Shock Wave (Formirovaniya pogranichnogo sloya na plastine s dvizhushchimsya skachkom uplotneniya). Prikladnaya Matematika i Mekhanika, No. 3, 1957.
2. Bromberg, R. Use of the Shock Tube Wall Boundary Layer in Heat Transfer Studies. Jet Propulsion, 26, No. 9, 737-740, 1956. Translation from the English in "Mekhanika", No. 3, IL, 1957.
3. Present-Day State of the Aerodynamics of Supersonic Velocities. Edited by Khouart, Vol. 1. Translated from the English, IL, 1955.
4. Mirels, H. The Wall Boundary - Layer Behind a Moving Shock Wave. Boundary Layer Research (Grenzschichtforschung). Berlin, p. 283-293, ill. Bill. 21, 1958.
5. Lykov, A.V. Theory of Thermal Conductivity (Teoriya teploprovodnosti). Gostekhteoretizdat, 1952.
6. Gordon, Hall J., Hertzberg, A. Recent Advances in Transient Surface Temperature Thermometry. ARS-J. Vol. 28, No. 11, November, 1958.